

Article

# A Numerical Solution and Comparative Study of the Symmetric Rossler Attractor with the Generalized Caputo Fractional Derivative via Two Different Methods

Mohamed Elbadri <sup>1,2</sup>, Mohamed A. Abdoon <sup>3,4</sup>, Mohammed Berir <sup>4,5</sup> and Dalal Khalid Almutairi <sup>6,\*</sup>

<sup>1</sup> Department of Mathematics, Faculty of Sciences and Arts, Jouf University, Tubarjal 74713, Saudi Arabia; badry19822@gmail.com

<sup>2</sup> Department of Mathematic, University of Gezira, Wad Madani 21111, Sudan

<sup>3</sup> Department of Basic Sciences (Mathematics), Deanship of Preparatory Year, Shaqra University, Riyadh 15342, Saudi Arabia; moh.abdoon@gmail.com

<sup>4</sup> Department of Mathematics, Faculty of Science, Bakht Al-Ruda University, Duwaym 999129, Sudan; midriss@bu.edu.sa

<sup>5</sup> Department of Mathematics, Faculty of Science and Arts, Al-Baha University, Baljurashi 1988, Saudi Arabia

<sup>6</sup> Department of Mathematics, College of Education (Majmaah), Majmaah University, Al-Majmaah 11952, Saudi Arabia

\* Correspondence: dk.almutairi@mu.edu.sa

**Abstract:** This study focuses on the solution of the rotationally symmetric Rossler attractor by using the adaptive predictor–corrector algorithm (Apc-ABM-method) and the fractional Laplace decomposition method ( $\rho$ -Laplace DM). Furthermore, a comparison between the proposed methods and Runge–Kutta Fourth Order (RK4) is made. It is discovered that the proposed methods are effective and yield solutions that are identical to the approximate solutions produced by the other methods. Therefore, we can generalize the approach to other systems and obtain more accurate results. In addition to this, it has been shown to be useful for correctly discovering examples via the demonstration of attractor chaos. In the future, the two methods can be used to find the numerical solution to a variety of models that can be used in science and engineering applications.

**Keywords:** numerical solution; the Apc-ABM method;  $\rho$ -Laplace DM; generalized Caputo fractional derivative

**MSC:** 26A33; 44A10; 65P20



**Citation:** Elbadri, M.; Abdoon, M.A.; Berir, M.; Almutairi, D.K. A Numerical Solution and Comparative Study of the Symmetric Rossler Attractor with the Generalized Caputo Fractional Derivative via Two Different Methods. *Mathematics* **2023**, *11*, 2997. <https://doi.org/10.3390/math11132997>

Academic Editor: Alicia Cordero

Received: 9 June 2023

Revised: 30 June 2023

Accepted: 3 July 2023

Published: 5 July 2023



**Copyright:** © 2023 by the authors. Licensee MDPI, Basel, Switzerland. This article is an open access article distributed under the terms and conditions of the Creative Commons Attribution (CC BY) license (<https://creativecommons.org/licenses/by/4.0/>).

## 1. Introduction

In recent decades, fractional differential equations have become prominent due to modeling and chaos [1,2]. Many alternative approaches to solving fractional differential equations have been developed [3,4]. Many fields, from electrical engineering to biology and physics, have found use for the modeling of chaotic and hyper-chaotic systems [5–8].

Numerous studies cover chaos application: the modeling of electrical circuits. The use of chaotic models is acceptable because of how difficult it is to forecast a wide range of real-world occurrences. Numerous novel methods for assessing chaotic systems have appeared in recent years [9–12]. Two of these methods, asymptotic stability and Lyapunov exponents, shed light on how the parameters of the model affect the dynamics of the chaotic model. Numerous mathematical and scientific fields make use of fractional calculus. For certain cutting-edge research and applications, scientists, mathematicians, biologists, and those from other fields [13–19] are increasingly turning to fractional calculus. Given the ambiguity surrounding fractional operators, this finding is noteworthy. Singularity freedom [20] applies to derivatives with exponential and Mittag–Leffler kernels. Since they consider the impact of long-term memory, the fractional derivatives are very useful.

In this study, we use methods to analyze numerical solutions to chaotic systems with generalized fractional derivative orders. By using a rigorous mathematical methodology, we explore cutting-edge and time-saving approaches to the problem of solving the new fractional chaotic model. As a result, there is hope for the investigation of further models using the proposed techniques.

In [21–23], Katugampola introduced the generalized fractional integral and the fractional derivative. The generalization of the definition of the fractional derivative with Caputo type is given in [24].

The researchers introduced the fractional Laplace transform to deal with generalized fractional derivatives [25]. It was used to solve some mathematical problems involving generalized fractional derivatives. A coupling of the fractional Laplace transform and some other analytical methods [26,27] was used to solve problems containing a generalized fractional derivative. The results indicated the effectiveness of these methods. One such effective method is the  $\rho$ -Laplace decomposition method ( $\rho$ -Laplace DM), which has been used to solve differential equations involving a generalized fraction.

There are many strong reasons to use fractional derivatives in practice. The fractional Rössler system, a set of three nonlinear equations that displays chaotic dynamics, is an extension of the original Rössler system. Some possible physical or chemical phenomena that the fractional Rössler system could describe are a chemical reaction's fluid flow dynamics and a chaotic oscillator's dynamics with fractional damping [28], as proven by recent studies [29–31]. The literature contains many examples of chaotic systems, such as the Lorenz attractor, the electrical circuit described by Chua, the system described by Chen, the system described by Lu, and the basic chaotic system [32–36].

Systems that have symmetry are more susceptible to multistability because it is guaranteed that each asymmetric attractor will have a twin attractor that is symmetrical with it. Due to the fact that every asymmetric attractor contains a symmetric twin attractor, systems that have symmetry are particularly susceptible to the phenomenon of multistability. However, there is a possibility that there are advantages to multistability, such as the capacity to recreate and research events in the actual world, where they also exist. Consider the rotationally symmetric Rossler attractor [37], which is described by

$$\begin{aligned} D_0^{\alpha,\rho} x(t) &= -y - yz, \\ D_0^{\alpha,\rho} y(t) &= x + ay, \\ D_0^{\alpha,\rho} z(t) &= b + z(x^2 - c), \end{aligned} \quad (1)$$

where  $D_0^{\alpha,\rho}(\cdot)$  is the generalized Caputo-type fractional derivative [24],  $a=0.4$ ,  $b=0.4$ ,  $c=4.5$ , and the system is chaotic, with initial conditions  $x(0) = 1.5$ ,  $y(0) = 0.0$ , and  $z(0) = 0.0$ .

The prospect of multistability is offered by chaotic dynamical systems that have a symmetric structure thanks to the presence of an independent amplitude control parameter. The development of symmetric Rossler systems results in the production of a symmetric pair of unusual attractors that coexist together. In chaotic systems, symmetry offers a unique amplitude control parameter that may be used independently, which is beneficial for engineering applications.

This study focuses on the solution of the rotationally symmetric Rossler attractor by using two different methods. We are able to apply the methods to various types of systems in order to obtain more accurate findings. We are certain that our approaches will be used in the not-too-distant future to design and simulate a wide range of fractional models. These models have the potential to be utilized in the resolution of increasingly difficult physics, biology, and engineering issues.

The significance of these techniques rests in the fact that they are used to find a numerical solution in a variety of models, including disease models and chaotic models, and that it can be expanded to incorporate other models in pathology, dynamical models, coding, and hyper-chaos. Both capabilities contribute to the method's overall usefulness.

In addition to this, the method is useful for the discovery of chaos and can be applied to other, more complex models.

**2. Basic Definitions**

**Definition 1.** The generalized fractional integral of the function  $f$ ,  $I_{a+}^{\alpha,\rho} f(t)$ ,  $\alpha > 0$ , and  $\rho > 0$ , is given by

$$I_{a+}^{\alpha,\rho} f(t) = \frac{\rho^{1-\alpha}}{\Gamma(\alpha)} \int_a^t s^{\rho-1} (t^\rho - s^\rho)^{\alpha-1} f(s) ds, \quad \alpha > 0, t > a, \tag{2}$$

for  $m - 1 < \alpha \leq m$ , where  $m \in \mathbb{N}$  (see [21]).

**Definition 2.** The generalized Riemann–Liouville fractional derivative (RLFD) of the function  $f$ ,  ${}^R D_{a+}^{\alpha,\rho} f(t)$ , of order  $\alpha > 0$ , is given by [22].

$${}^R D_{a+}^{\alpha,\rho} f(t) = \frac{\rho^{\alpha-m+1}}{\Gamma(m-\alpha)} \left( t^{1-\rho} \frac{d}{dt} \right)^m \int_a^t s^{\rho-1} (t^\rho - s^\rho)^{m-\alpha-1} f(s) ds, \quad t > a \geq 0. \tag{3}$$

**Definition 3.** The generalized Caputo fractional derivative (CFD) operator,  $\mathcal{D}_{a+}^{\alpha,\rho}$ ,  $\alpha > 0$ , is given by

$$\left( \mathcal{D}_{a+}^{\alpha,\rho} f \right) (t) = \frac{\rho^{\alpha-m+1}}{\Gamma(m-\alpha)} \int_a^t s^{\rho-1} (t^\rho - s^\rho)^{m-\alpha-1} \left( s^{1-\rho} \frac{d}{ds} \right)^m f(s) ds, \quad t > a. \tag{4}$$

where  $\rho > 0, a \geq 0$ , and  $m - 1 < \alpha < m$  (see [24]).

**Definition 4 ([25]).** The  $\rho$ -Laplace transform of a function  $f : [0, \infty) \rightarrow \mathbb{R}$  is defined by

$$L_\rho \{ f(t) \} = \int_0^\infty e^{-\delta \frac{t^\rho}{\rho}} f(t) \frac{dt}{t^{1-\rho}}. \tag{5}$$

The  $\rho$ -Laplace transform of the generalized CFD is defined by

$$L_\rho \left\{ \mathcal{D}_0^{\alpha,\rho} f(t) \right\} = \delta^\alpha L_\rho \{ f(t) \} - \delta^{\alpha-1} f(0). \tag{6}$$

**3. Methodology of the Apc-ABM Algorithm**

The purpose of this part is to present the algorithm used in the APC-ABM method:

$$\begin{cases} \mathcal{D}_{a+}^{\alpha,\rho} y(t) = f(t, y(t)), & t \in [0, T], \\ y^{(k)}(a) = y_0^k, & k = 0, 1, \dots, [\alpha], \end{cases} \tag{7}$$

where  $\mathcal{D}_{a+}^{\alpha,\rho}$  is a generalized Caputo fractional operator.

Then, for  $n - 1 < \alpha \leq n, a > 0, \rho > 0, y \in C^n([a, T])$ , model (8) is equivalent and we obtain

$$y(t) = u(t) + \frac{\rho^{1-\alpha}}{\Gamma(\alpha)} \int_a^t s^{\rho-1} (t^\rho - s^\rho)^{\alpha-1} f(s, y(s)) ds, \tag{8}$$

where

$$u(t) = \sum_{n=0}^{m-1} \frac{1}{\rho^n n!} (t^\rho - a^\rho)^n \left[ \left( x^{1-\rho} \frac{d}{dx} \right)^n y(x) \right] \Big|_{x=a}. \tag{9}$$

The first step of our algorithm, under the assumption that the function  $f$  is such that a unique solution exists on some interval  $[a, T]$ , consists of dividing the interval  $[a, T]$  into  $N$  unequal subintervals,  $\{[t_k, t_{k+1}], k = 0, 1, \dots, N - 1\}$ , using the mesh points.

$$\begin{cases} t_0 = a, \\ t_{k+1} = \left(t_k^\rho + h\right)^{1/\rho}, k = 0, 1, \dots, N - 1, \end{cases} \tag{10}$$

where  $h = \frac{T^\rho - a^\rho}{N}$ . Now, to numerically solve the IVPs, we build approximations  $y_k, k = 0, 1, \dots, N$ . If we have previously assessed the approximations  $y(t_j)$  and  $y_j \approx y(t_j) (j = 1, 2, \dots, k)$ , we wish to use the integral equation to generate the approximation  $y_{k+1} \approx y(t_{k+1})$ .

$$y(t_{k+1}) = u(t_{k+1}) + \frac{\rho^{1-\alpha}}{\Gamma(\alpha)} \int_a^{t_{k+1}} s^{\rho-1} \left(t_{k+1}^\rho - s^\rho\right)^{\alpha-1} f(s, y(s)) ds, \tag{11}$$

Making the substitution

$$z = s^\rho \tag{12}$$

we obtain

$$y(t_{k+1}) = u(t_{k+1}) + \frac{\rho^{-\alpha}}{\Gamma(\alpha)} \int_{a^\rho}^{t_{k+1}^\rho} \left(t_{k+1}^\rho - z\right)^{\alpha-1} f\left(z^{1/\rho}, y\left(z^{1/\rho}\right)\right) dz \tag{13}$$

That is,

$$y(t_{k+1}) = u(t_{k+1}) + \frac{\rho^{-\alpha}}{\Gamma(\alpha)} \sum_{j=0}^k \int_{t_j^\rho}^{t_{j+1}^\rho} \left(t_{k+1}^\rho - z\right)^{\alpha-1} f\left(z^{1/\rho}, y\left(z^{1/\rho}\right)\right) dz \tag{14}$$

Subsequently, the trapezoidal quadrature method is employed in consideration of the weight function  $\left(t_{k+1}^\rho - z\right)^{\alpha-1}$ . In order to estimate the integrals on the right-hand side of the equation, a suitable method must be employed (Equation (13)). The corrector formula is derived in the following manner,  $y(t_{k+1}), k = 0, 1, 2, \dots, N - 1$ :

$$y(t_{k+1}) \approx u(t_{k+1}) + \frac{\rho^{-\alpha} h^\alpha}{\Gamma(\alpha + 2)} \sum_{j=0}^k a_{j,k+1} f(t_j, y(t_j)) + \frac{\rho^{-\alpha} h^\alpha}{\Gamma(\alpha + 2)} f(t_{k+1}, y(t_{k+1})) \tag{15}$$

where

$$a_{j,k+1} = \begin{cases} k^{\alpha+1} - (k - \alpha)(k + 1)^\alpha & \text{if } j = 0, \\ (k - j + 2)^{\alpha+1} + (k - j)^{\alpha+1} - 2(k - j + 1)^{\alpha+1} & \text{if } 1 \leq j < k \end{cases} \tag{16}$$

The ultimate step of our methodology involves substituting the quantity  $y(t_{k+1})$ . The predictor value is located on the right-hand side of Formula (15),  $y^P(t_{k+1})$ . The integral equation (Equation (13)) is solved through the utilization of the one-step Adams–Bashforth method. In this scenario, the act of replacing the function with another equivalent one is considered.  $f\left(z^{1/\rho}, y\left(z^{1/\rho}\right)\right)$  at each integral in Equation (16) with the amount  $f(t_j, y(t_j))$  yields

$$y^P(t_{k+1}) \approx u(t_{k+1}) + \frac{\rho^{-\alpha}}{\Gamma(\alpha)} \sum_{j=0}^k \int_{t_j^\rho}^{t_{j+1}^\rho} \left(t_{k+1}^\rho - z\right)^{\alpha-1} f(t_j, y(t_j)) dz \tag{17}$$

$$y^P(t_{k+1}) = u(t_{k+1}) + \frac{\rho^{-\alpha} h^\alpha}{\Gamma(\alpha + 1)} \sum_{j=0}^k [(k + 1 - j)^\alpha - (k - j)^\alpha] f(t_j, y(t_j)) \tag{18}$$

Thus, the aforementioned formula comprehensively characterizes our adaptive P-C approach for evaluating the approximation,  $y_{k+1} \approx y(t_{k+1})$ :

$$y_{k+1} \approx u(t_{k+1}) + \frac{\rho^{-\alpha} h^\alpha}{\Gamma(\alpha + 2)} \sum_{j=0}^k a_{j,k+1} f(t_j, y_j) + \frac{\rho^{-\alpha} h^\alpha}{\Gamma(\alpha + 2)} f\left(t_{k+1}, y_{k+1}^P\right), \tag{19}$$

where  $y_j \approx y(t_j), j = 0, 1, \dots, k$ , and the predicted value  $y_{k+1}^P \approx y^P(t_{k+1})$  can be determined as described in Equation (18) with the weights  $a_{j,k+1}$  being defined according to (35). The proposed adaptive Apc-ABM-method uses a non-uniform grid  $\{t_{j+1} = (t_j^\rho + h)^\rho : j = 0, 1, \dots, N - 1\}$  with  $t_0 = a$  and  $h = \frac{T^\rho - a^\rho}{N}$ , where  $N$  represents a positive integer. It is posited that the utilization of the Apc-ABM methodology for initial value problems (IVPs) featuring the generalized CFD is rendered infeasible in instances where a uniform grid is employed, as is the case with the aforementioned scenario [38].

#### 4. Applications of the Apc-ABM Algorithm

This section is dedicated to exploring the solutions of Equation (1). With the Apc-ABM method, great results can be achieved when  $a = b = 0.4$  and  $c = 4.5$ , with initial conditions  $x(0) = 1.5, y(0) = 0$ , and  $z(0) = 0$ . By using Equation (18), the approximations  $x_{k+1}, y_{k+1}$ , and  $z_{k+1}$ , and for  $N \in \mathbb{N}$  and  $T > 0$ ,

$$\begin{cases} x_{k+1} \approx x_0 + a \frac{\rho^{-\alpha} h^\alpha}{\Gamma(\alpha+2)} \sum_{j=0}^k a_{j,k+1} (y_j - x_j) + a \frac{\rho^{-\alpha} h^\alpha}{\Gamma(\alpha+2)} (y_{k+1}^P - x_{k+1}^P), \\ y_{k+1} \approx y_0 + \frac{\rho^{-\alpha} h^\alpha}{\Gamma(\alpha+2)} \sum_{j=0}^k a_{j,k+1} ((c - a)x_j - x_j z_j + cy_j) + \frac{\rho^{-\alpha} h^\alpha}{\Gamma(\alpha+2)} ((c - a)x_{k+1}^P - x_{k+1}^P z_{k+1}^P + cy_{k+1}^P), \\ z_{k+1} \approx z_0 + \frac{\rho^{-\alpha} h^\alpha}{\Gamma(\alpha+2)} \sum_{j=0}^k a_{j,k+1} (x_j y_j - bz_j) + \frac{\rho^{-\alpha} h^\alpha}{\Gamma(\alpha+2)} (x_{k+1}^P y_{k+1}^P - bz_{k+1}^P), \end{cases} \quad (20)$$

where  $h = \frac{T^\rho}{N}$  and

$$\begin{cases} x_{k+1}^P \approx x_0 + a \frac{\rho^{-\alpha} h^\alpha}{\Gamma(\alpha+1)} \sum_{j=0}^k [(k + 2 - 1 - j)^\alpha + (-k + j)^\alpha] (y_j - x_j), \\ y_{k+1}^P \approx y_0 + \frac{\rho^{-\alpha} h^\alpha}{\Gamma(\alpha+1)} \sum_{j=0}^k [(k + 2 - 1 - j)^\alpha + (-k + j)^\alpha] ((c - a)x_j - x_j z_j + cy_j), \\ z_{k+1}^P \approx z_0 + \frac{\rho^{-\alpha} h^\alpha}{\Gamma(\alpha+1)} \sum_{j=0}^k [(k + 2 - 1 - j)^\alpha + (-k + j)^\alpha] (x_j y_j - bz_j). \end{cases} \quad (21)$$

Table 1 presents the numerical solution using the Apc-ABM method to Equation (21) when  $\alpha = 1, \rho = 1, (a, b, c) = (0.5, 0.5, 3.5)$ , and  $(x_0, y_0, z_0) = (1/2, 1/2, 0)$ , and comparing the results with the RK4 method. Table 2 presents the numerical solution for the value of  $\alpha = 0.95$ .

**Table 1.** Numerical solutions for a fractional equation (Equation (1)) when  $\alpha = 1, \rho = 1, N = 200$ , and  $t = 2$ .

$h$	$x$	$y$	$z$
1/160	-1.439249004245022	1.926879753830334	0.115497632553681
1/320	-1.437027804276252	1.919749862274107	0.115546731072315
1/640	-1.435904100808411	1.916191943945559	0.115570069443809
1/1280	-1.435338988519151	1.914414758678336	0.115581435786859
1/2560	-1.435055619161782	1.913526611637655	0.115587043236967
1/5120	-1.434913731421401	1.913082649779714	0.115589828030596
1/10240	-1.434842736816009	1.912860696799313	0.115591215694437
1/20480	-1.434780588799649	1.912666503235824	0.115592427311921
R K4	-1.434770838159845	1.912637598049335	0.115592614892760

**Table 2.** Numerical solutions for a fractional equation (Equation (1)) when  $\alpha = 0.95, \rho = 1$ , and  $t = 0.5$ .

$h$	$x$	$y$	$z$
1/160	1.28921526386768	0.794012894194367	0.113077179858054
1/320	1.287865984843871	0.793856954812710	0.112751179833214

**Table 2.** Cont.

<i>h</i>	<i>x</i>	<i>y</i>	<i>z</i>
1/640	1.287192129056913	0.793776634317518	0.112588754203015
1/1280	1.286855399733513	0.793735886510549	0.112507684690222
1/2560	1.286687085043668	0.793715365736676	0.112467185722739
1/5120	1.286602940232841	0.793705068634685	0.112446945181642
1/10240	1.286560870966092	0.793699910905249	0.112436827146182
1/20480	1.286524062075699	0.793695392872633	0.112427975087295
R K4	1.286518803332891	0.793694747080276	0.112426709876828

**5.  $\rho$ -Laplace DM**

In this section, we discuss Equation (7) with a generalized CFD to illustrate the algorithm of the  $\rho$ -Laplace DM.

The  $\rho$ -Laplace DM divides Equation (1) into a linear term  $Ay(t)$ , a nonlinear term  $By(t)$ , and a source function  $C(t)$  as follows:

$$D_0^{\alpha,\rho} y(t) = Ay(t) + By(t) + C(t), \rho > 0, 0 < \alpha \leq 1, \tag{22}$$

Taking  $L_\rho$  to Equation (22), we obtain

$$L_\rho[y(t)] = \frac{y_0}{\delta} + \frac{1}{\delta^\alpha} L_\rho[C(t)] + \frac{1}{\delta^\alpha} L_\rho[Ay(t) + By(t)] \tag{23}$$

Operating  $L_\rho^{-1}$ , we obtain

$$y(t) = G(t) + L_\rho^{-1} \left[ \frac{1}{\delta^\alpha} L_\rho[Ay(t) + By(t)] \right] \tag{24}$$

where  $G(t) = L_\rho^{-1} \left[ \frac{y_0}{\delta} + \frac{1}{\delta^\alpha} L_\rho[C(t)] \right]$ .

The  $\rho$ -Laplace DM represents a series solution of  $y(t)$  by

$$y(t) = \sum_{n=0}^{\infty} y_n(t) \tag{25}$$

Furthermore, the nonlinear function  $By(t)$  can be expressed in a series of polynomials:

$$\sum_{n=0}^{\infty} K_n \tag{26}$$

Substituting Equations (25) and (26) into Equation (24) yields

$$\sum_{n=0}^{\infty} y_n(t) = G(t) + L_\rho^{-1} \left[ \frac{1}{\delta^\alpha} L_\rho \left[ A \sum_{n=0}^{\infty} y_n(t) + \sum_{n=0}^{\infty} K_n \right] \right]. \tag{27}$$

As a result, the recurrence relation

$$y_0(\tau) = G(t), \tag{28}$$

$$y_{n+1}(\tau) = L_\rho^{-1} \left[ \frac{1}{\delta^\alpha} L_\rho [Ay_n(t) + K_n] \right], n \geq 0. \tag{29}$$

Finally, a series is used to approximate the solution.

$$\psi_M(t) = \sum_{n=0}^{M-1} y_n(t) \tag{30}$$

### 6. Application of $\rho$ -Laplace DM

According to what is presented in Section 5, after applying the  $\rho$ -Laplace DM to each equation of System (1), we obtain

$$\begin{aligned} \sum_{n=0}^{\infty} x_n(t) &= x(0) + L_{\rho}^{-1} \left[ \frac{1}{\delta^{\alpha}} L_{\rho} \left[ - \sum_{n=0}^{\infty} y_n(t) - \sum_{n=0}^{\infty} U_n \right] \right] \\ \sum_{n=0}^{\infty} y_n(t) &= y(0) + L_{\rho}^{-1} \left[ \frac{1}{\delta^{\alpha}} L_{\rho} \left[ \sum_{n=0}^{\infty} x_n(t) - a \sum_{n=0}^{\infty} y_n(t) \right] \right], \\ \sum_{n=0}^{\infty} z_n(t) &= \frac{bt^{\alpha\rho}}{\rho^{\alpha}\Gamma[1+\alpha]} + L_{\rho}^{-1} \left[ \frac{1}{\delta^{\alpha}} L_{\rho} \left[ \sum_{n=0}^{\infty} V_n - c \sum_{n=0}^{\infty} z_n(t) \right] \right]. \end{aligned} \tag{31}$$

where the nonlinear terms  $yz$  and  $zx^2$  are given by

$$yz = \sum_{n=0}^{\infty} U_n \text{ and } yz = \sum_{n=0}^{\infty} U_n \tag{32}$$

The  $\rho$ -Laplace DM provides the recursive relation:

$$\begin{aligned} x_0(t) &= 1.5 \\ y_0(t) &= 0 \\ z_0(t) &= \frac{bt^{\alpha\rho}}{\rho^{\alpha}\Gamma[1+\alpha]} \\ x_{n+1}(t) &= L_{\rho}^{-1} \left[ \frac{1}{\delta^{\alpha}} L_{\rho} [-y_n(t) - U_n(t)] \right], n \geq 0 \\ y_{n+1}(t) &= L_{\rho}^{-1} \left[ \frac{1}{\delta^{\alpha}} L_{\rho} [x_n(t) - ay_n(t)] \right], n \geq 0 \\ z_{n+1}(t) &= L_{\rho}^{-1} \left[ \frac{1}{\delta^{\alpha}} L_{\rho} [V_n(t) - cz_n(t)] \right], n \geq 0 \end{aligned}$$

The first few components are

$$\begin{aligned} x_0(t) &= 1.5 \\ y_0(t) &= 0 \\ z_0(t) &= \frac{bt^{\alpha\rho}\rho^{-\alpha}}{\Gamma[1+\alpha]} \\ x_1(t) &= 0 \\ y_1(t) &= \frac{1.5t^{\rho\alpha}\rho^{-\alpha}}{\Gamma[1+\alpha]} \\ z_1(t) &= \frac{b(2.25 - c)t^{2\rho\alpha}\rho^{-2\alpha}}{\Gamma[1+2\alpha]} \\ x_2(t) &= -\frac{1.5bt^{3\alpha\rho}\rho^{-3\alpha}\Gamma[1+2\alpha]}{\Gamma^2[1+\alpha]\Gamma[1+3\alpha]} - \frac{1.5t^{2\alpha\rho}\rho^{-2\alpha}}{\Gamma[1+2\alpha]} \\ y_2(t) &= \frac{1.5at^{2\alpha\rho}\rho^{-2\alpha}}{\Gamma[1+2\alpha]} \\ z_2(t) &= \frac{b(5.0625 - 4.5c + c^2)t^{3\alpha\rho}\rho^{-3\alpha}}{\Gamma[1+3\alpha]} \end{aligned}$$

$$x_3(t) = -\frac{1.5at^{3\alpha\rho}\rho^{-3\alpha}}{\Gamma[1+3\alpha]} - \frac{1.5b(2.25-c)\Gamma[1+3\alpha]t^{4\alpha\rho}\rho^{-4\alpha}}{\Gamma[1+\alpha]\Gamma[1+2\alpha]\Gamma[1+4\alpha]} - \frac{1.5ab\Gamma[1+3\alpha]t^{4\alpha\rho}\rho^{-4\alpha}}{\Gamma[1+\alpha]\Gamma[1+2\alpha]\Gamma[1+4\alpha]}$$

$$y_3(t) = -\frac{1.5t^{3\alpha\rho}\rho^{-3\alpha}}{\Gamma[1+3\alpha]} + \frac{1.5a^2t^{3\alpha\rho}\rho^{-3\alpha}}{\Gamma[1+3\alpha]} - \frac{1.5bt^{4\alpha\rho}\rho^{-4\alpha}\Gamma[1+2\alpha]}{\Gamma^2[1+\alpha]\Gamma[1+4\alpha]}$$

Therefore, the approximate solution is given as

$$\begin{aligned} x(t) &= \sum_{n=0}^{\infty} x_n(t), \\ y(t) &= \sum_{n=0}^{\infty} y_n(t), \\ z(t) &= \sum_{n=0}^{\infty} z_n(t). \end{aligned} \tag{33}$$

Table 3 displays the  $\rho$ -Laplace DM solution of Equation (1). When  $\alpha = 0.90$  and  $\rho = 0.95$ , we observed that the  $\rho$ -Laplace DM solution given in Table 3 for the fractional order and fractional parameter has the same behavior as the  $\rho$ -Laplace DM solution given in Table 4 for integers  $\alpha = 1$  and  $\rho = 1$ .

**Table 3.**  $\rho$ -Laplace DM solutions to fractional model equation (Equation (1)) when  $\alpha = 0.90$  and  $\rho = 0.95$ .

$t$	$x$	$y$	$z$
0	1.5	0.0	0.0
0.1	1.4796996703743301	0.2347426924022824	0.05053705282095178
0.2	1.430966701161987	0.4315761993664601	0.07795664830887342
0.3	1.3578018024536942	0.6161357560230636	0.09178543190387903
0.4	1.2621444225163563	0.7907363746739074	0.09111861049966521
0.5	1.145647714788557	0.9552091317148814	0.07230353761707926

**Table 4.** A comparison of the numerical solutions to fractional model equation (Equation (1)).

$t$	$x$ - $\rho$ -Laplace D	$x$ - Apc-ABM	$x$ - RK4
0	1.5	1.5	1.5
0.1	1.492213875	1.492219789642530	1.492218810160190
0.2	1.467822	1.467899837621127	1.467897787108336
0.3	1.4255238749999999	1.425901742914282	1.425898584622672
0.4	1.3643519999999998	1.365527369775399	1.365523123300982
0.5	1.283671875	1.286524062075699	1.286518803332891
$t$	$y$ - $\rho$ -Laplace D	$y$ - Apc-ABM	$y$ - RK4
0	0.0	0.0	0.0
0.1	0.15278500000000003	0.152780418545565	0.152780702318047
0.2	0.31024000000000007	0.310175637425140	0.310176020055442
0.3	0.47092500000000001	0.470625099220481	0.470625370691797
0.4	0.63328000000000002	0.632410659829444	0.632410592018532
0.5	0.79562499999999999	0.793695392872633	0.793694747080276
$t$	$z$ - $\rho$ -Laplace D	$z$ - Apc-ABM	$z$ - RK4
0	0.0	0.0	0.0
0.1	0.035795535625	0.035799537976347	0.035799091697084
0.2	0.06402089000000001	0.064132733630666	0.064131982855701
0.3	0.085135625625	0.085961681371914	0.085960705651558
0.4	0.09848848	0.101893186504205	0.101892039586943
0.5	0.102259765625	0.112427975087295	0.112426709876828



Table 4 also shows the comparison of outcomes of the solution of system (1) using the  $\rho$ -Laplace DM, Apc-ABM method, and RK4 method when  $\alpha = 1, \rho = 1, a = b = 0.4,$  and  $c = 4.5,$  with  $x(0) = 1.5, y(0) = 0,$  and  $z(0) = 0.$  We note that the results obtained when using the  $\rho$ -Laplace DM and Apc-ABM methods are very close to those obtained using the RK4 method.

In Figures 1 and 2, solutions were drawn using Equation (1) by using the Apc-ABM-method, with  $(a, b, c) = (0.2, 0.2, 6.5), (x_0, y_0, z_0) = (1, 0, 0), T = 400,$  and  $N = 800$  when  $\alpha = 0.95$  and  $\rho = 0.8, 1.2.$  In Figure 3, solutions were drawn using Equation (1) by using  $\alpha = 1$  and  $\rho = 1.$

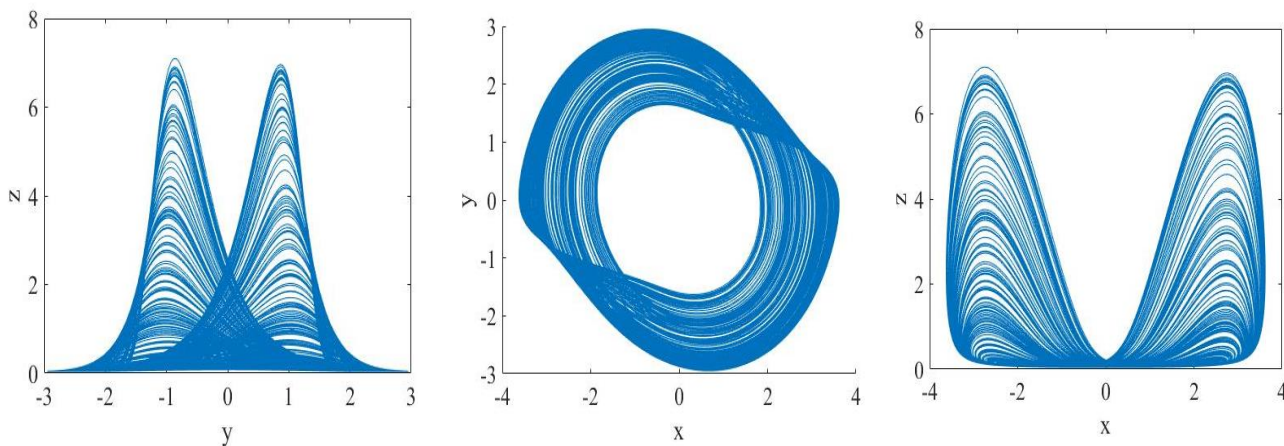


Figure 1. Chaotic attractor of Equation (1), when  $\alpha = 0.95$  and  $\rho = 0.8.$

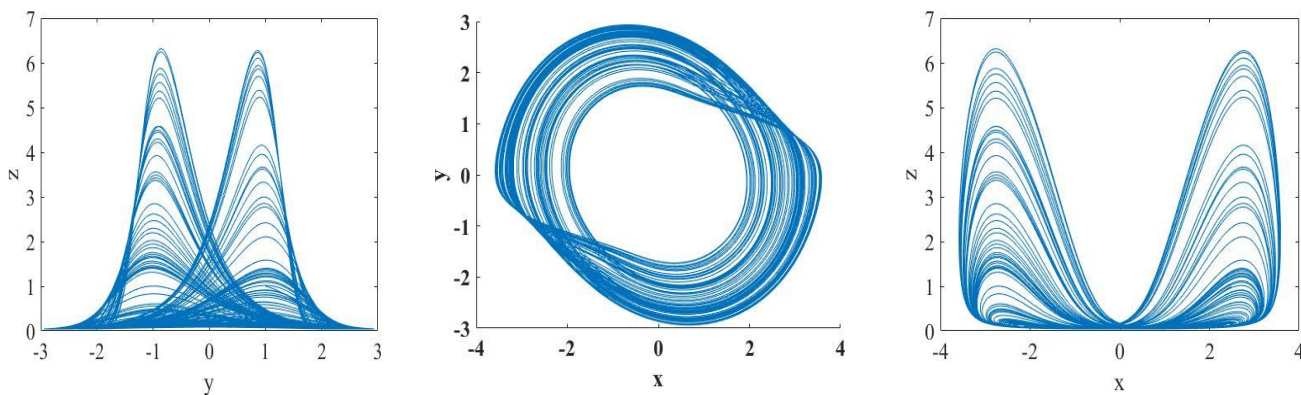


Figure 2. Chaotic attractor of Equation (1), when  $\alpha = 0.95$  and  $\rho = 1.2.$

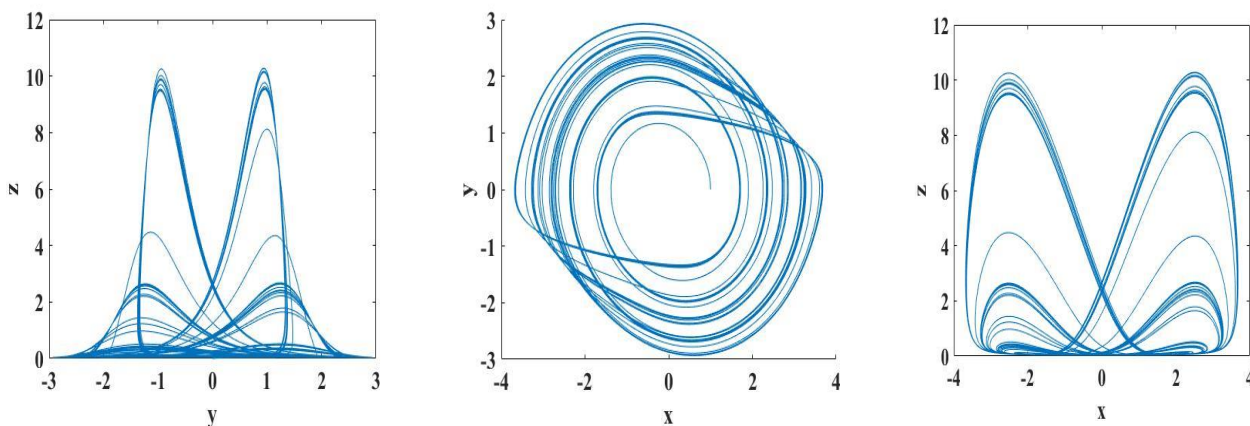


Figure 3. Chaotic attractor of Equation (1), when  $\alpha = 1$  and  $\rho = 1.$

## 7. Conclusions

This study presents the numerical solution of a fractional system using two different methods and compares the solutions. The APc-ABM method and the  $\rho$ -Laplace DM both benefited from the provision of a numerical strategy that was accomplished with the help of software packages. As the step size  $h$  fell, the APc-ABM technique produced numerical results that were impressively close to the RK4 solutions. Furthermore, we showed from the comparison that the numerical solutions obtained by the Laplace DM and APc-ABM are identical to the approximate solutions produced by the RK4 method. The obtained numerical results demonstrate that our method carries out its procedures in the context of fractions in a way that satisfies expectations with regard to the degree to which it maintains its numerical stability. We suggest applying this strategy to more complex physics and engineering problems.

**Author Contributions:** Methodology, M.E., M.A.A. and D.K.A.; Software, M.B. All authors have read and agreed to the published version of the manuscript.

**Funding:** This research received no external funding.

**Data Availability Statement:** No data were used to support this study.

**Acknowledgments:** The authors would like to thank the Deanship of Scientific Research at Majmaah University for supporting this work.

**Conflicts of Interest:** The authors declare no conflict of interest.

## References

- Podlubny, I. *Fractional Differential Equations*; Academic Press: New York, NY, USA, 1999.
- Oldham, K.B.; Spanier, J. *The Fractional Calculus*; Academic Press: New York, NY, USA, 1974.
- Carpinteri, A.; Mainardi, F. (Eds.) *Fractals and Fractional Calculus in Continuum Mechanics*; Springer: Wien, Austria; New York, NY, USA, 1997; pp. 277–290.
- Samko, G.; Kilbas, A.; Marichev, O. *Fractional Integrals and Derivatives: Theory and Applications*; Gordon and Breach: Amsterdam, The Netherlands, 1993.
- Dudkowski, D.; Jafari, S.; Kapitaniak, T.; Kuznetsov, N.V.; Leonov, G.A.; Prasad, A. Hidden Attractors in Dynamical Systems. *Phys. Rep.* **2016**, *637*, 1–50. [[CrossRef](#)]
- Xu, G.; Shekofteh, Y.; Akgül, A.; Li, C.; Panahi, S. A New Chaotic System with a Self-Excited Attractor: Entropy Measurement, Signal Encryption, and Parameter Estimation. *Entropy* **2018**, *20*, 86. [[CrossRef](#)]
- Lai, Q.; Akgül, A.; Li, C.; Xu, G.; Çavuşoğlu, Ü. A New Chaotic System with Multiple Attractors: Dynamic Analysis, Circuit Realization and S-Box Design. *Entropy* **2017**, *20*, 12. [[CrossRef](#)] [[PubMed](#)]
- Petráš, I. A Note on the Fractional-Order Chua's System. *Chaos Solitons Fractals* **2006**, *38*, 140–147. [[CrossRef](#)]
- Abdoon, M.A.; Hasan, F.L.; Taha, N.E. Computational Technique to Study Analytical Solutions to the Fractional Modified KDV-Zakharov-Kuznetsov Equation. *Abstr. Appl. Anal.* **2022**, *2022*, 2162356. [[CrossRef](#)]
- Abd El-Maksoud, A.J.; Abd El-Kader, A.A.; Hassan, B.G.; Rihan, N.G.; Tolba, M.F.; Said, L.A.; Radwan, A.G.; Abu-Elyazeed, M.F. FPGA Implementation of Sound Encryption System Based on Fractional-Order Chaotic Systems. *Microelectronics* **2019**, *90*, 323–335. [[CrossRef](#)]
- Ahmed, S.A.; Elzaki, T.M.; Elbadri, M.; Mohamed, M.Z. Solution of Partial Differential Equations by New Double Integral Transform (Laplace—Sumudu Transform). *Ain Shams Eng. J.* **2021**, *12*, 4045–4049. [[CrossRef](#)]
- Sene, N. Global Asymptotic Stability of the Fractional Differential Equations. *J. Nonlinear Sci. Its Appl.* **2019**, *13*, 171–175. [[CrossRef](#)]
- Singh, J.; Kumar, D.; Hammouch, Z.; Atangana, A. A Fractional Epidemiological Model for Computer Viruses Pertaining to a New Fractional Derivative. *Appl. Math. Comput.* **2017**, *316*, 504–515. [[CrossRef](#)]
- Kumar, S.; Kumar, R.; Cattani, C.; Samet, B. Chaotic Behaviour of Fractional Predator-Prey Dynamical System. *Chaos Solitons Fractals* **2020**, *135*, 109811. [[CrossRef](#)]
- Hammouch, Z.; Mekkaoui, T.; Belgacem, F.B.M. Numerical Simulations for a Variable Order Fractional Schnakenberg Model. *AIP Conf. Proc.* **2014**, *1637*, 1450–1455.
- Abdoon, M.A.; Saadeh, R.; Berir, M.; Guma, F.E. Analysis, Modeling and Simulation of a Fractional-Order Influenza Model. *Alex. Eng. J.* **2023**, *74*, 231–240. [[CrossRef](#)]
- Hammouch, Z.; Mekkaoui, T. Traveling-wave solutions of the generalized Zakharov equation with time-space fractional derivatives. *Math. Eng. Sci. Aerosp.* **2014**, *5*, 489–498.
- Belgacem, F.B.M.; Silambarasan, R.; Zakia, H.; Mekkaoui, T. New and Extended Applications of the Natural and Sumudu Transforms: Fractional Diffusion and Stokes Fluid Flow Realms. In *Trends in Mathematics*; Springer: Singapore, 2017; pp. 107–120.

19. Toufik, M.; Atangana, A. New Numerical Approximation of Fractional Derivative with Non-Local and Non-Singular Kernel: Application to Chaotic Models. *Eur. Phys. J. Plus* **2017**, *132*, 444. [[CrossRef](#)]
20. Behzad Ghanbari, D. Abdon Atangana, Some New Edge Detecting Techniques Based on Fractional Derivatives with Nonlocal and Non-Singular Kernels. *Adv. Differ. Equ.* **2020**, *2020*, 435. [[CrossRef](#)]
21. Katugampola, U.N. New Approach to a Generalized Fractional Integral. *Appl. Math. Comput.* **2011**, *218*, 860–865. [[CrossRef](#)]
22. Katugampola, U.N. A New Approach to Generalized Fractional Derivatives. *Bull. Math. Anal. Appl.* **2014**, *6*, 1–15.
23. Katugampola, U.N. Existence and Uniqueness Results for a Class of Generalized Fractional Differential Equations. *arXiv* **2014**, arXiv:1411.5229v2, preprint.
24. Almeida, R.; Malinowska, A.B.; Odziejewicz, T. Fractional Differential Equations with Dependence on the Caputo–Katugampola Derivative. *J. Comput. Nonlinear Dyn.* **2016**, *11*, 061017. [[CrossRef](#)]
25. Jarad, F.; Abdeljawad, T. A modified Laplace transform for certain generalized fractional operators. *Results Nonlinear Anal.* **2018**, *1*, 88–98.
26. Sene, N.; Fall, A.N. Homotopy Perturbation  $\rho$ -Laplace Transform Method and Its Application to the Fractional Diffusion Equation and the Fractional Diffusion-Reaction Equation. *Fractal Fract.* **2019**, *3*, 14. [[CrossRef](#)]
27. Elbadri, M. Initial Value Problems with Generalized Fractional Derivatives and Their Solutions via Generalized Laplace Decomposition Method. *Adv. Math. Phys.* **2022**, *2022*, 3586802. [[CrossRef](#)]
28. Rysak, A.; Sedlmayr, M.; Gregorczyk, M. Revealing Fractionality in the Rössler System by Recurrence Quantification Analysis. *Eur. Phys. J. Spec. Top.* **2023**, *232*, 83–98. [[CrossRef](#)]
29. Qazza, A.; Abdoon, M.; Saadeh, R.; Berir, M.A. New Scheme for Solving a Fractional Differential Equation and a Chaotic System. *Eur. J. Pure Appl. Math.* **2023**, *16*, 1128–1139. [[CrossRef](#)]
30. Saadeh, R.; AAbdoon, M.; Qazza, A.; Berir, M. A Numerical Solution of Generalized Caputo Fractional Initial Value Problems. *Fractal Fract.* **2023**, *7*, 332. [[CrossRef](#)]
31. Elbadri, M.; Abdoon, M.A.; Berir, M.; Almutairi, D.K. A Symmetry Chaotic Model with Fractional Derivative Order via Two Different Methods. *Symmetry* **2023**, *15*, 1151. [[CrossRef](#)]
32. Elbadri, M.; Ahmed, S.A.; Abdalla, Y.T.; Hdidi, W. A New Solution of Time-Fractional Coupled KdV Equation by Using Natural Decomposition Method. *Abstr. Appl. Anal.* **2020**, *2020*, 3950816. [[CrossRef](#)]
33. Sene, N. Mathematical Views of the Fractional Chua’s Electrical Circuit Described by the Caputo-Liouville Derivative. *Rev. Mex. Fis.* **2021**, *67*, 91–99. [[CrossRef](#)]
34. Morin, O.; Gillis, A.; Chen, J.; Aubin, M.; Bucci, M.K.; Roach, M., 3rd; Pouliot, J. Megavoltage Cone-Beam CT: System Description and Clinical Applications. *Med. Dosim. Off. J. Am. Assoc. Med. Dosim.* **2005**, *31*, 51–61. [[CrossRef](#)]
35. Zhang, D.; Lu, G. Review of Shape Representation and Description Techniques. *Pattern Recognit.* **2004**, *37*, 1–19. [[CrossRef](#)]
36. Zhang, X.; Wang, C.; Yao, W.; Lin, H. Chaotic System with Bondorbital Attractors. *Nonlinear Dyn.* **2019**, *97*, 2159–2174. [[CrossRef](#)]
37. Li, C.; Hu, W.; Sprott, J.C.; Wang, X. Multistability in Symmetric Chaotic Systems. *Eur. Phys. J. Spec. Top.* **2015**, *224*, 1493–1506. [[CrossRef](#)]
38. Odibat, Z.; Baleanu, D. Numerical Simulation of Initial Value Problems with Generalized Caputo-Type Fractional Derivatives. *Appl. Numer. Math. Trans. IMACS* **2020**, *156*, 94–105. [[CrossRef](#)]

**Disclaimer/Publisher’s Note:** The statements, opinions and data contained in all publications are solely those of the individual author(s) and contributor(s) and not of MDPI and/or the editor(s). MDPI and/or the editor(s) disclaim responsibility for any injury to people or property resulting from any ideas, methods, instructions or products referred to in the content.